Article

Chitosan Nanoparticles, a Novel Drug Delivery System to Transfer Squalene for Hepatocyte Stress Protection

Seyed Hesamoddin Bidooki, Lea Spitzer, Arnaud Petitpas, Javier Sánchez-Marco,
Roberto Martínez-Beamonte, Roberto Lasheras, Virginie Pellerin, María J. Rodríguez-Yoldi,
María Angeles Navarro, Jesús Osada,* and Susana C. M. Fernandes*

Read Online

ACCESS | Metrics & More | Article Recommendations | SI Supporting Information

ABSTRACT: The Mediterranean diet is a well-known dietary pattern that has gained considerable popularity worldwide for its ability to prevent the progression of nonalcoholic fatty liver disease. This is largely attributed to the use of virgin olive oil as the primary source of fat, which contains a substantial amount of squalene, a natural antioxidant. In order to enhance the delivery of squalene and amplify its effects due to its highly hydrophobic nature, herein, squalene has been incorporated into chitosan nanoparticles. The characterization of the resulting nanoparticles was conducted via scanning electron microscopy, dynamic light scattering, ζ potential, Fourier transform infrared spectroscopy, and gas chromatography−mass spectrometry. Reactive oxygen species (ROS) generation and cell viability assays were conducted in oxidative and endoplasmic reticulum (ER) stress in AML12 and a TXNDC5-deficient AML12 cell line, which was generated by CRISPR/Cas9 technology. The results demonstrated that squalene was successfully encapsulated in chitosan nanoparticles and exhibited rapid and efficient cellular uptake at a 150 μM squalene concentration within 48 h. In conclusion, the encapsulation of squalene in chitosan nanoparticles, compared to the poly(D,L-lactide-co-glycolic acid) and ethanol drug carriers, significantly enhanced its cellular uptake. This allows the administration of higher doses, which improve hepatocyte viability and reduce ROS levels, effectively compensating for the adverse effects of TXNDC5 deficiency under the context of hepatocyte stress protection.
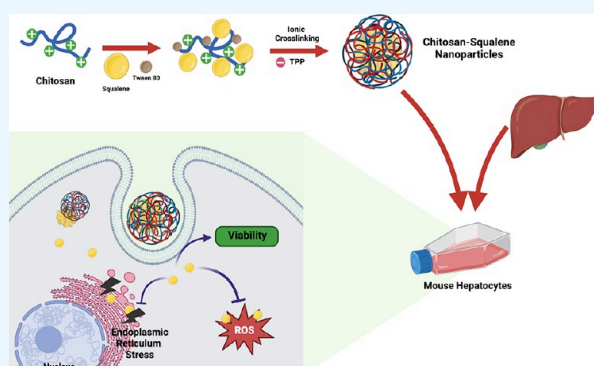
1. INTRODUCTION

Metabolic disease is a growing societal burden, leading to increased morbidity and mortality rates due to subsequent cardiovascular disease and cancer.[1] As a multifactorial metabolic disorder, nonalcoholic fatty liver disease (NAFLD) affects approximately 30% of the general population and is currently the most common liver disease in Western countries.[2] NAFLD develops naturally in the absence of alcohol abuse and initially presents as simple steatosis, which is the abnormal accumulation of lipids in the liver and eventually, it progresses to cirrhosis.[2,3] The Mediterranean diet is a well-known dietary pattern worldwide and has become popular for preventing the progression of NAFLD.[4,5] This dietary pattern includes a variety of plant-based foods, such as fruits, vegetables, nuts, and in particular olive oil.[5] The consumption of virgin olive oil has been associated with a reduced risk of general and cause-specific mortality in cardiovascular disease.[6] Virgin olive oil is high in monounsaturated fatty acids, particularly oleic acid, and other minor bioactive components including squalene which is a major unsaponifiable component, contributing to its anti-inflammatory and antioxidant properties.[5−8]

Squalene (SQ) is a terpenoid hydrocarbon that is widely present in nature (Figure 1). It can be found in substantial amounts in virgin olive oil, although the richest source of squalene is shark liver oil, which has been traditionally used as a source of this lipid.[9] Squalene is an intermediate in the biosynthesis of phytosterols in plants or cholesterol in animals.[10] It is synthesized in all types of cells because it is a key intermediate in the formation of eukaryotic sterols and bacterial hopanoids.[10] Squalene has several beneficial properties. It is a natural antioxidant and serves to hydrate the skin. Additionally, it is extensively used as an excipient in pharmaceutical formulations for disease management and therapy due to its biocompatibility, inertness, and other advantageous properties. Furthermore, it has been found to have a preventive effect on breast cancer and possesses tumor-
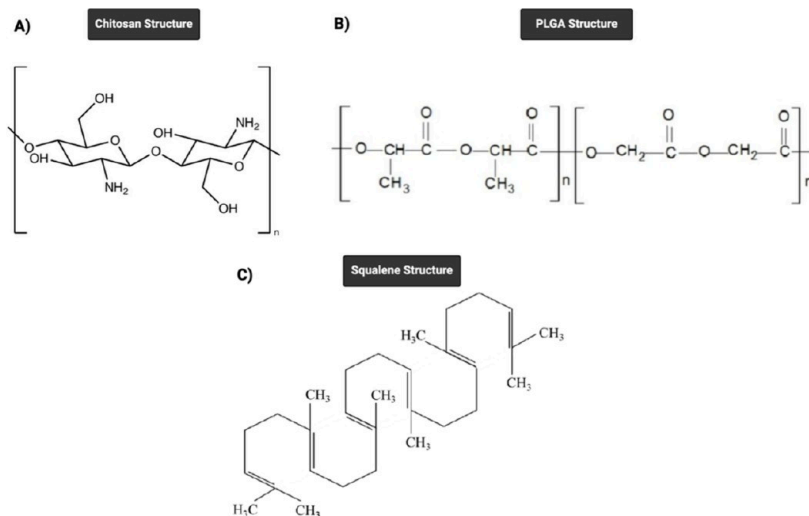
Figure 1. Chemical structures of (A) chitosan, (B) PLGA, and (C) squalene.

protective and cardio-protective properties.[10] It also decreases serum cholesterol levels.[10,11] Although squalene is a weak inhibitor of tumor cell proliferation, it has a potentiation effect that contributes to the treatment of cancer, either directly or indirectly.[11] Additionally, squalene is being investigated for vaccine delivery applications due to its ability to enhance the immune response to various associated antigens. These qualities make squalene a potentially interesting excipient for therapeutic applications.[11] Due to its high degree of unsaturation, squalene is susceptible to oxidation by a number of factors, including oxygen, temperature, moisture content, metals, and light. If squalene can be effectively encapsulated, it can be preserved without affecting the chemical and sensory attributes of the final product.[12] The administration of squalene has been demonstrated to reduce hepatic fat content and to induce the expression of proteins involved in lipid metabolism, which may result in reduced endoplasmic reticulum (ER) stress and intracellular reactive oxygen species (ROS) levels.[5] Thioredoxin domain-containing 5 (TXNDC5), a protein located in the ER, protects hepatocytes from stress-induced apoptosis by participating in protein modification and folding, and performs vital roles in antioxidative harm, antianoxia-induced apoptosis and cellular proliferation.[13]

Nanoparticles (NPs) have been demonstrated to offer superior performance to alternative drug delivery technologies, including enhanced circulation time, increased solubility for hydrophobic drugs, and targeted drug delivery.[14,15] The use of nanoparticles to encapsulate anticancer therapy and other disorder-specific compounds has been extensively studied with the objective of protecting sensitive chemicals from degradation, thus enhancing their bioavailability. Consequently, a plethora of naturally derived and biodegradable particles, including chitosan (CS), poly(D,L-lactide-co-glycolic acid) (PLGA) (Figure 1), and protein-based particles, have been developed.

PLGA is a particularly efficacious biodegradable polymer, as its hydrolysis results in the generation of endogenous monomer metabolites, namely lactic acid and glycolic acid. These monomers can be effectively degraded within the body via the Krebs cycle. Therefore, the low risk of systemic toxicity in PLGA applications such as drug delivery and tissue engineering can be attributed to the aforementioned factors.[5] Conversely, CS is employed as an encapsulation agent for a multitude of sensitive substances, including hydrophobic and lipophilic drugs, vitamins, astaxanthin, fish oil, and curcumin, among others.[12,16,17] CS is a modified natural polysaccharide obtained by the partial N-deacetylation of chitin, a natural biopolymer derived from the exoskeleton of crustaceans, including crabs, shrimps, and lobsters.[18−21] CS is soluble in aqueous acidic media and can be produced in a variety of molecular weights and with different degrees of deacetylation.[18,22] CS possesses a wide range of bioactivities, including antioxidant, antimicrobial, antifungal, antitumor, antiallergic, immune system activating, antihypertensive, and cholesterol-lowering properties.[12,15,23−27] Chitosan nanoparticles (CSNPs), with diameters ranging from 1 to 1,000 nm, have been widely used therapeutically as drug carriers, wherein the active ingredient is dissolved, entrapped, encapsulated, adsorbed, or chemically bound due to their biodegradability, biocompatibility and nontoxicity.[18,28−30] CSNPs possess the advantage of a slow and controlled drug release, which improves drug solubility and stability, enhances efficacy, and reduces toxicity. Due to their small size, they are capable of passing through biological barriers in vivo (such as the blood-brain barrier) and delivering drugs to the lesion site, thereby enhancing efficacy.[14]

In this context, the present study focuses on the preparation and characterization of CSNPs as a drug delivery system to enhance the therapeutic effect of squalene followed by its administration to hepatocytes. The cellular uptake of CSNP-squalene and the effects of initial squalene content, encapsulation efficiency, and mean particle size were also investigated. In comparison to alternative methodologies such as PLGA-squalene nanoparticles, the antioxidant properties of squalene have been examined using this innovative drug delivery system, particularly in the context of ER and oxidative stress. Furthermore, this investigation was conducted in the absence of TXNDC5 protein, which serves as a target gene.

2. MATERIALS AND METHODS

2.1. Materials. Low molecular weight chitosan (LMw CS) and high molecular weight chitosan (HMw CS) were obtained from Sigma-Aldrich/Merck Millipore (Darmstadt, Germany) and Mahtani Chitosan Pvt. Ltd. (India), respectively. The following materials were purchased from Sigma-Aldrich/Merck

Millipore (Darmstadt, Germany): acetic acid, Tween 80, sodium tripolyphosphate (TPP), squalene (2.05 M, ≥98%, liquid), Resomer RG 503H poly(D,L-lactide-co-glycolic acid) (PLGA-COOH), ethanol, and ethyl acetate 99.6% ACS. Pluronic F68 was procured from Panreac Química S. L. U. (Barcelona, Spain). Cyclohexane was supplied by VWR (Radnor, Pennsylvania, USA).

The mouse hepatocyte cell line (AML12) was procured from the ATCC collection (Manassas, VA, USA). Dulbecco's modified Eagle's minimum essential medium (DMEM), fetal bovine serum, nonessential amino acids, amphotericin B, penicillin, streptomycin, trypsin, EDTA, and the Lipofectamine 2000 kit were obtained from Thermo Fisher Scientific (Waltham, MA, USA). The following materials were obtained from Sigma-Aldrich/Merck Millipore (Darmstadt, Germany): dexamethasone, 5α-cholestane, 3-(4,5-dimethylthiazol-2-yl)-2,5-diphenyltetrazolium bromide assay (MTT), hydrogen peroxide (H_2O_2), thapsigargin, dimethyl sulfoxide (DMSO), palmitic acid, and 2,7-dichlorofluorescein diacetate (DCFH-DA). F-12 Ham's medium was purchased from GE Healthcare Life Science (South Logan, UT, USA), and insulin-transferrin-selenium was obtained from Corning (Bedford, MA, USA). TXNDC5 CRISPR/Cas9 KO plasmids were provided by Santa Cruz Biotechnology (Dallas, TX, USA).

2.2. Preparation and Characterization of the Nanoparticles.

2.2.1. Synthesis of Squalene-Loaded Chitosan Nanoparticles.

Chitosan nanoparticles (CSNPs) were synthesized by the ionic gelation and ultrasonication approaches, as previously published.[12,16,31,32] Two different chitosan samples were used: (i) LMw CS with a Mw range of 50−190 kDa and a degree of deacetylation (DDA) range of 75−85% from Sigma-Aldrich, Merck Millipore (Darmstadt, Germany); and (ii) HMw CS presenting an average Mw of 500 kDa (determined by viscosimetry) and a DDA of 98% (determined by ^1H NMR spectroscopy in D_2O containing a 1% of CD_3COOD) and processed to medical grade from Mahtani Chitosan Pvt. Ltd. (India).

Briefly, 1 mg/mL solution was first prepared by dissolving chitosan (LMw CS or HMw CS) in aqueous acetic acid (1% v/v) at room temperature under vigorous stirring for 48 h. After, Tween 80 (0.5% v/v) (Sigma-Aldrich, Merck Millipore, Darmstadt, Germany) were added to the chitosan solution and the solution was filtered through a 0.45 μm filter and the pH adjusted to 4.5 with NaOH 1M. To this solution, 0.5 mg/mL of sodium tripolyphosphate (TPP, Sigma-Aldrich; Merck Millipore, Darmstadt, Germany) solution, prepared with double-distilled water (pH adjusted to 4.5 with HCl 1M) and filtered through a 0.45 μm filter, was added dropwise under stirring (CS:TPP ratio = 2.5:1). The solution was then sonicated using a Branson Digital Sonifier 450 (Danbury, CT, USA) in an ice bath for 25 s at 80% amplitude using a 2 mm diameter probe. The mixture was then stirred for cross-linking under a fume hood at 600 rpm for 3 h. Finally, the nanoparticles were collected by centrifugation (Thermo Fisher Scientific, Waltham, MA, USA) at 15,000 g for 15 min at 10 °C and dispersed in 2 mL of double-distilled water for subsequent cellular experiments. The preparation of chitosan-squalene nanoparticles (CS-SQ NPs) involved the dispersion of squalene (2.05 M, ≥98%, liquid; Sigma-Aldrich, Merck Millipore, Darmstadt, Germany) into CS-TPP solution. The solution was prepared with the different volumes of squalene (50, 100, and 200 μL) under stirring. The mixtures were then sonicated for 25 s and 80% amplitude in an ice bath, and

stirred for 3 h. The unreacted chemicals and byproducts were removed by centrifugation (15,000g for 15 min at 10 °C). The final samples were stored at 4 °C in the dark prior to analysis.

2.2.2. Physicochemical and Morphological Characterization of the Chitosan Nanoparticles.

The size, polydispersity index (PDI) and zeta potential of the nanoparticles were studied using the Malvern Zetasizer Nano ZS coupled to an MPT-2 auto titrator system (Malvern Instruments, Worcester, UK). The size reported is the z-average diameter (intensity based) of five measurements by Dynamic Light Scattering (DLS) at 25 °C and 90° scattering angle.

The chemical composition of the starting and final materials, such as pure squalene and squalene encapsulated with LMw or HMw chitosan, were confirmed using Attenuated Total Reflectance Fourier Transform Infrared (ATR-FTIR) spectroscopy on a Nicolet iS50 (ThermoFisher Scientific, Waltham, Massachusetts, USA) from wavenumber 400−4000 cm^{-1} with a resolution of 4 cm^{-1} and an accumulation of 64 scans.

The morphological features of CSNPs and CS-SQ NPs were analyzed using an Apreo 2 Scanning Electron Microscope (SEM, ThermoFisher Scientific, Waltham, MA, USA) operating at an acceleration voltage of 30 kV with a Scanning Transmission Electron Microscopy (STEM) detector. Prior to SEM analysis, the samples were coated with a thin layer of gold (Au) using a sputter coater (Cressington 108 Auto Sputter Coater, Watford, UK) to enhance conductivity and image resolution. For STEM analysis, NPs were dispersed in ultrapure water to obtain a suspension with a very low concentration. The mixture was then subjected to a sonication bath for 3 min. A 2 μL droplet of the sonicated suspension was placed on a 200 mesh Cu TEM grid type B (Ted Pella Inc., Redding, California, USA), and excess water was evaporated from the grid overnight under a fume hood at room temperature before being placed in the STEM chamber for morphological studies.

2.2.3. Chitosan Encapsulation Efficiency Experiment.

CSNPs with different initial squalene volumes (200, 100, 50 μL of 2.05 M squalene) were synthesized and then washed twice with water using an ultrafiltration device (Amicon, molecular weight cutoff, 100 000 Da). Squalene was extracted from the NPs using cyclohexane and was then quantified by gas chromatography−mass spectrometry (GC/MS), as described in the Squalene Extraction subsection. The drug loading content (DLC) and encapsulation efficiency (EE) of the LMw CSNP and HMw CSNP were calculated according to the following equations:[32]

$$DLC = \frac{\text{Weight of squalene in nanoparticles}}{\text{Chitosan nanoparticles weight}}$$

$$EE\ (\%) = \frac{\text{Total squalene added} - \text{Nonentrapped squalene}}{\text{Total squalene added}} \times 100$$

2.2.4. Synthesis and Characterization of Squalene-Loaded PLGA Nanoparticles.

PLGA-Squalene polymeric nanoparticles (PLGA-SQ NPs) were synthesized for comparison with CS-SQ NPs by the single emulsion solvent evaporation technique using Resomer RG 503H poly(D,L-lactide-co-glycolic acid) (PLGA-COOH, Mw 24−38 kDa) (Sigma-Aldrich; Merck Millipore, Darmstadt, Germany), Pluronic F68 (Panreac Química S. L.U; Barcelona, Spain)

and ethyl acetate 99.6% ACS (Sigma-Aldrich, Merck Millipore, Darmstadt, Germany) as described previously.[5] A scanning electron microscope (SEM, FEG INSPECT-F50, Eindhoven, Netherlands), transmission electron microscopy (TEM) (Tecnai T20, FEI Company, Hillsboro, OR, USA) and DLS (Malvern Instruments, Worcester, UK) were used to determine the physicochemical characterization of these nanoparticles.

2.2.5. Preparation of Ethanol−Squalene System. An ethanol-squalene system (Eth-SQ) was prepared for comparison with CS-SQ NPs by the solvent displacement technique.[33,34] Squalene (2.05 M, ≥98%, liquid; Sigma-Aldrich, Merck Millipore, Darmstadt, Germany) was initially dissolved in 100% ethanol (Sigma-Aldrich; Merck Millipore, Darmstadt, Germany) to attain the requisite concentration. Subsequently, the squalene-ethanol solution was introduced to the cell culture medium, thereby enabling the dispersion of the squalene within the medium following the evaporation of the ethanol. The resulting squalene dispersion was then directly applied to the cells for the purpose of conducting biological experiments.

2.2.6. Viscosity Measurement. The viscosity of the drug delivery systems was quantified using the MCR302 DG23.04 Pressure Cell C-PDT200 (Anton Paar, Graz, Austria) with a bucket and cylinder (bucket diameter = 20.33 mm, cylinder diameter = 21.04 mm). All measurements were conducted at a temperature of 25 °C. For the purpose of measuring viscosity, approximately 3 mL of each sample was collected and subsequently loaded onto the rheometer. The viscosity of the nanoparticles was determined in accordance with the manufacturer's instructions.

2.3. Biological Assays. *2.3.1. AML12 Cell Culture.* The mouse hepatocyte cell line (AML12) (ATCC collection, Manassas, VA, USA) was cultured in 25 cm^2 plastic flasks at a density of 5×10^5 cells/cm^2 (in duplicate) at 37 °C in a humidified atmosphere of 5% CO_2 in Dulbecco's modified Eagle's minimum essential medium (DMEM; Thermo Fisher Scientific, Waltham, MA, USA): F-12 Ham's medium (GE Healthcare Life Science, South Logan, UT, USA) at a 1:1 ratio supplemented with 10% fetal bovine serum (Thermo Fisher Scientific, Waltham, MA, USA), 1:500 insulin-transferrin-selenium (Corning, Bedford, MA, USA), 40 ng/mL dexamethasone (Sigma-Aldrich; Merck Millipore, Darmstadt, Germany), 1% nonessential amino acids (Thermo Fisher Scientific, Waltham, MA, USA), 1% amphotericin B (1000 mg/mL; Thermo Fisher Scientific, Waltham, MA, USA), 1% penicillin (1000 U/mL; Thermo Fisher Scientific, Waltham, MA, USA), and 1% streptomycin (1000 mg/mL; Thermo Fisher Scientific, Waltham, MA, USA). The culture medium was changed every 2 days. After the AML12 cells reached 90−100% confluence, the medium was removed and the cells were washed with PBS and trypsinized with 0.25% trypsin (DMEM; Thermo Fisher Scientific, Waltham, MA, USA) and 1 mM EDTA (DMEM; Thermo Fisher Scientific, Waltham, MA, USA).

2.3.2. Generating a Stable TXNDC5 Knockout AML12 Cell Line. The stable TXNDC5-deficient clones were expanded as described previously.[5] Briefly, AML12 cells were transfected with TXNDC5/ERp46 HDR and TXNDC5 CRISPR/Cas9 KO plasmids (Santa Cruz Biotechnology, Dallas, TX, USA) using Lipofectamine 2000 (Thermo Fisher Scientific, Waltham, MA, USA). The gRNA sequence 5′-TTATCAAG-TTCTTCGCTCCG-3′ in the TXNDC5 CRISPR/Cas9 KO

plasmid caused a double-strand break in the fifth exon of Txndc5. AML12 KO cells that were resistant to puromycin were selected after repeated puromycin incubations. Finally, the absence of TXNDC5 was confirmed by Western blot.

2.3.3. Cellular Uptake Assay. AML12 cells were seeded in 25 cm^2 plastic flasks at a density of 5×10^5 cells/cm^2 (in triplicate) in complete growth medium. After the cells reached 90% confluence, they were treated with CS-SQ NPs, PLGA-SQ NPs or Eth-SQ at two different concentrations (30 and 150 μM) and two different incubation time (48 and 72 h) in medium without fetal bovine serum and amphotericin B. The cells were then trypsinized and washed three times with PBS, pH 7.4 and centrifuged at 3900 rpm for 5 min and collected for squalene extraction.

2.3.4. Squalene Extraction. Squalene was extracted from CS-SQ NPs, PLGA-SQ NPs and cells treated with different drug delivery systems, and analyzed by GC/MS as previously described.[35] Briefly, according to the weight of the samples and the volumes used in each step, the samples were transferred to a centrifuge glass tube and homogenized in 1 mL of PBS, 10 μL of 1 mM 5α-cholestane (Sigma-Aldrich; Merck Millipore, Darmstadt, Germany) in cyclohexane (VWR, Radnor, Pennsylvania, USA) as an internal standard to determine the efficiency of the extraction and 1 mL of cyclohexane and vortexed for 10 s. After centrifugation, the organic phase was transferred to a clean tube. The eluted samples were dried with a nitrogen gas in a thermostatic bath at 55 °C. They were then dissolved in 200 μL of 50 μM squalane solution (Sigma-Aldrich; Merck Millipore, Darmstadt, Germany) in cyclohexane for chromatographic analysis. CG analyses were performed in an Agilent 6890 CG with a 7683B injector and a 5975B MS acquisition parameter unit (Agilent Technologies, Santa Clara, CA, USA), using a J&W122-5532 column (Agilent) with a nominal length of 30 m and a diameter of 0.25 mm and a helium flow of 1 mL/min. The oven temperature was set to run from 280 to 290 °C in 15 min with a ramp from 5 to 13 min.

2.3.5. Cell Viability Assay. Cellular viability was determined using the 3-(4 5-dimethylthiazol-2-yl)-2 5-diphenyltetrazolium bromide assay (MTT; Sigma-Aldrich, Merck Millipore, Darmstadt, Germany).[36] Cells were seeded on a 96-well plate at 5000 cells/well and exposed for 24, 48, and 72 h to the range of 15 to 600 μM CS-SQ NPs diluted in medium without fetal bovine serum and amphotericin B. In another assay, cells after treatment with 150 μM CS-SQ NPs were exposed for 24 h to 8 mM H_2O_2 (Sigma-Aldrich, Merck Millipore, Darmstadt, Germany) for oxidative stress, 12.5 nM thapsigargin (Sigma-Aldrich, Merck Millipore, Darmstadt, Germany) dissolved in DMSO and 600 μM palmitic acid (Sigma-Aldrich, Merck Millipore, Darmstadt, Germany) dissolved in ethanol for ER stress. Then, 1 mg/mL MTT was added to the culture medium. After 3 h of incubation, the cell growth medium was replaced with DMSO and the absorbance was measured with a SPECTROstar Nano Microplate Reader (Omega, BMG Labtech, Ortenberg, Germany) at 570 nm.

2.3.6. Reactive Oxygen Species Assay. AML12 cells (5000 cells per well) were seeded in a 96-well plate and cultured at 37 °C for 72 h. Cells were treated with CS-SQ NPs or CSNPs diluted in medium without fetal bovine serum and amphotericin B at a concentration of 150 μM for 48 h, followed by treatment with 8 mM H_2O_2 (Sigma-Aldrich, Merck Millipore, Darmstadt, Germany), 12.5 nM thapsigargin (Sigma-Aldrich, Merck Millipore, Darmstadt, Germany)

dissolved in DMSO or 600 μM palmitic acid (Sigma-Aldrich, Merck Millipore, Darmstadt, Germany) dissolved in ethanol. 10 μL of 2.0 mg/mL 2,7-dichlorofluorescein diacetate (DCFH-DA; Sigma-Aldrich, Merck Millipore, Darmstadt, Germany) dissolved in fresh PBS was added to the cells. After 3 h, the medium was removed and the presence of ROS was assessed by measuring the conversion of DCFH-DA to fluorescent dichlorofluorescein (DCF) at excitation and emission wavelengths of 485 and 520 nm, respectively, in a microplate reader (FLUOstar, Omega, BMG Labtech, Ortenberg, Germany).

2.3.7. Characterization of Cell Morphology in the Presence of Chitosan, PLGA, and Ethanol Drug Delivery Systems. Both WT and KO AML12 cells (2000 cells per well) were cultured in a 12-well plate (in duplicate). Cells were incubated for 48 h in the presence of 150 μM CS-SQ NPs and uncharged CSNPs as control, 150 μM PLGA-SQ NPs and uncharged PLGA NPs as control, and 150 μM Eth-SQ and ethanol as control. After three washes with PBS, a Floid Cell Imaging System (Thermo Fisher Scientific, Waltham, MA, USA) was used to detect the influence of different drug delivery systems on the AMl12 cell line.

2.3.8. Statistical Analysis. Statistical analyses were performed using GraphPad Prism 8 for Windows (GraphPad, San Diego, CA, USA). The Shapiro–Wilk test was used to determine the normal distribution of the data, and Bartlett's or Levene's test was used to determine the homology of variance between groups. Factors meeting both criteria were examined using one-way ANOVA with Dunnett's multiple comparison test and two-tailed Student's t test. If any of the hypotheses failed, statistical analysis was performed using the Mann–Whitney U test. A p-value of less than 0.05 was used to indicate statistical significance. Means and standard deviations of the results are presented.

3. RESULTS AND DISCUSSION

3.1. Encapsulation of Squalene in the Chitosan Nanoparticles.
Chitosan-based systems have found a multitude of applications in the food and biochemical industries due to their ability to encapsulate a wide range of ingredients.[37] The initial method described in the literature for the preparation of CSNPs involved emulsification and cross-linking. Herein, the CSNPs were prepared by the addition of a negatively charged TPP solution to a positively charged chitosan solution under magnetic stirring at room temperature followed by ultrasound approach.[38,39] Initial experiments were conducted using two chitosan samples with low and high molecular weights (LMw and HMw). As the biophysical characterization of PLGA-squalene was previously documented in our previous publication,[5] the particle size, surface charge, and EE% of all CSNPs were also evaluated and are presented in Table 1 and Table 2. The average diameter of LMw CSNPs

was 262.5 ± 80.1 nm, with a polydispersity index (PDI) of 0.35. However, HMw CSNPs exhibited an average diameter of 473.4 ± 62.3 nm and a PDI of 0.53. The increase in chitosan Mw resulted in an increase in the average particle size from 262 to 473 nm and PDI change from 0.35 to 0.53. These findings were consistent with previous observations that higher Mw chitosan produces larger nanoparticles.[19,40,41] The PDI was found to be low for all NPs evaluated, indicating that a homogeneous dispersion was obtained and it was observed that a higher variety of particle sizes were obtained when a solution of larger polymer chains was used. The positive charge of chitosan enables it to form a robust interaction with negatively charged molecules such as TPP, while maintaining its intrinsic activity.[42] Upon mixing chitosan and TPP, they spontaneously formed compact complexes with an overall positive surface charge of 20 ± 4 mV in LMw CSNPs and 35.5 ± 3 mV in HMw CSNPs, as confirmed by zeta potential measurements. In accordance with the literature, an analysis of the differences between the two CSNPs revealed a similar trend as observed for the particle size: a higher surface charge was obtained for particles formed by polymers with a longer chain.[43]

The size and PDI of a nanoparticle formulation have a significant impact on the loading and release of a drug.[44] Table 1 illustrates that the particle size and PDI of the developed CS-SQ NPs exhibited a range of 330.7 ± 77.4 nm with a 0.27 PDI in LMw CS-SQ NPs and 673.2 ± 38.8 nm with a 0.45 PDI in HMw CS-SQ NPs, which is conducive to passive targeting of tumors.[45] The results indicated that the CS-SQ NPs were comparatively larger than CSNPs, which is consistent with the findings of Keawchaoon and Yoksan using carvacrol.[46] The surface charge of CS-SQ NPs remained positive at 25 ± 6 mV and 40.9 ± 1.7 mV in LMw and HMw CS-SQ NPs, respectively. The positive surface charge of CS-SQ NPs is mainly due to the cationic nature of chitosan, which has protonated amine groups in aqueous solutions at neutral to slightly acidic pH. Squalene, which is hydrophobic, is encapsulated within the nanoparticle by hydrophobic interactions. Therefore, the positive surface charge is maintained due to the protonation of chitosan.[29]

FTIR analysis was conducted to confirm the encapsulation of squalene within the NPs (Figure 2). The various synthesized samples were studied in comparison with squalene and chitosan.[29] The ATR-FTIR spectra of the chitosan-squalene NPs revealed the presence of characteristic peaks at 2800–3000 cm^{-1}, which correspond to the C−H stretching of squalene,[47] and peaks at 1000–1100 cm^{-1}, which are indicative of the C−O−C vibration of chitosan. The selection of these peaks was based on their capacity to provide a qualitative measure of the encapsulation process. The C−H stretching bands of squalene were selected due to their pronounced intensity under the specified experimental conditions, providing a straightforward method for evaluating the relative quantity of squalene present in the nanoparticle system. While the C=C stretching (approximately 1640 cm^{-1}) was also a characteristic feature of squalene, the C−H stretching bands provided more discernible signals for monitoring the encapsulation process. Despite the fact that both chitosan and squalene display C−H stretching vibrations, the presence of squalene was substantiated by identifying specific C−H peaks that were exclusive to this compound in terms of wavenumber and intensity. These peaks were then validated by comparing them with individual and combined

Table 1. Diameter, Polydispersity Index (PDI), and Zeta Potential of Chitosan Nanoparticles without and with Squalene

Sample	Diameter (d.nm)	PDI	Zeta potential (mV)
LMw CSNPs	262.5 ± 80.1	0.35 ± 0.03	20 ± 4.0
HMw CSNPs	473.4 ± 62.3	0.53 ± 0.06	35.5 ± 3.0
LMw CS-SQ NPs	330.7 ± 77.4	0.27 ± 0.02	25 ± 6.0
HMw CS-SQ NPs	673.2 ± 38.8	0.45 ± 0.09	40.9 ± 1.7

Table 2. Squalene Content and Encapsulation Efficiency Based on the Squalene Initial Volume in LMw and HMw Chitosan Nanoparticles

Chitosan sample	Squalene initial volume	Squalene concentration (μM)	Squalene encapsulation (%)	Squalene/Chitosan (W/W)
LMw	200 μL	8015 ± 1065	61.5 ± 12.0	0.184
	100 μL	1838 ± 795	27.4 ± 3.0	0.042
	50 μL	1296 ± 676	38.9 ± 5.4	0.029
HMw	200 μL	1989 ± 247	14.7 ± 8.0	0.045
	100 μL	738 ± 335	11.3 ± 4.1	0.016
	50 μL	396 ± 290	13.2 ± 2.7	0.009
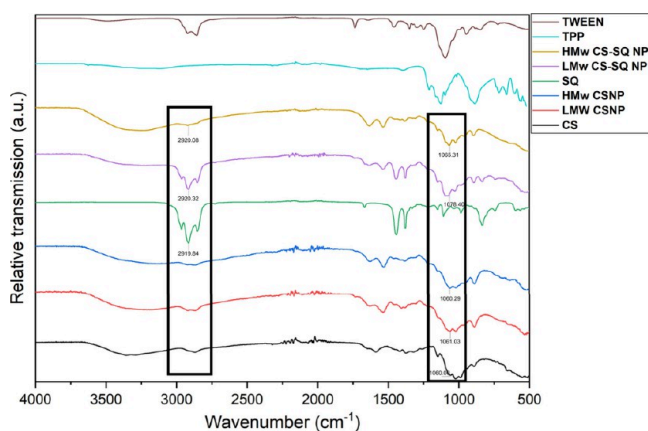
Figure 2. ATR-FTIR spectra of the different raw materials and chitosan-squalene nanoparticles. The black squares in Figure 2 indicate the typical peaks associated with the C−H stretching in the molecules of SQ and the C−O−C vibration bonds of CS, respectively. CS: chitosan. LMw CSNP: low molecular weight chitosan nanoparticle. HMw CSNP: high molecular weight chitosan nanoparticle. SQ: squalene. LMw CS-SQ NP: low molecular weight chitosan-squalene nanoparticle. HMw CS-SQ NP: high molecular weight chitosan-squalene nanoparticles. TPP: sodium tripolyphosphate. TWEEN: Tween 80. FTIR spectrum labels: broad O−H stretching (3200−3600 cm^{-1}), N−H stretching (3300−3500 cm^{-1}), C−H stretching (2800−3000 cm^{-1}), C=C stretching (1600−1680 cm^{-1}), C−O stretching (1000−1300 cm^{-1}), C−N stretching (1000−1350 cm^{-1}), C=O stretching (1650−1750 cm^{-1}), C−O−C stretching (900−1200 cm^{-1}).

spectra. This approach permitted the differentiation of the C−H stretching vibrations of squalene from those of chitosan within the CS-SQ NPs.[29,47] For chitosan, the C−O−C vibration (1000−1100 cm^{-1}) was selected as it is indicative of the glycosidic bond structure of the polysaccharide, thereby confirming its presence in the nanoparticles. Although other signals, such as the amide II band (around 1550 cm^{-1}) and the CO−H band (around 1410 cm^{-1}), are also characteristic of chitosan, the C−O−C peak enabled the reliable identification of chitosan within the system, without interference from other bands.[48]

By calculating the intensity ratios of squalene:chitosan bands (at 2800−3000 vs 1000−1100 cm^{-1}), we observed that the LMw CS-SQ NPs (0.8) exhibited a higher ratio than the HMw CS-SQ NPs (0.3), supporting our claim of higher encapsulation efficiency in LMw chitosan. These findings were consistent with the results of GC-MS, which indicated higher amounts of squalene in LMw CS-SQ NPs than the HMw CS-SQ NPs (Table 2), by using the equations provided in the experimental section. The maximum squalene loading in CSNPs was found to occur when using 200 μL of initial squalene volume, which reached 8015 ± 1065 μM of squalene

loading (Table 2). This corresponded to an encapsulation efficiency of 61.5 ± 12%. Among the tested formulations in our study, this represented the highest encapsulation efficiency achieved for squalene within chitosan nanoparticles. The encapsulation efficiency of squalene-loaded NPs has been reported in the literature to vary considerably, depending on the type of NP and the synthetic method employed, with values ranging from 26 to 82%.[12,49]

The results of this study confirmed that the LMw CSNPs with a positive charge have favorable properties for encapsulating squalene and could significantly influence their encapsulation efficiency of squalene. Consequently, these nanoparticles were selected for further investigation.

3.2. Morphology of the LMw Chitosan Nanoparticles.
SEM and scanning transmission electron microscopy in scanning electron microscopy (STEM in SEM) were employed to examine the morphology of the LMw NPs. Selected SEM and STEM in SEM micrographs of the CSNPs and CS-SQ NPs are presented in Figure 3A,B. As displayed in Figure 3A, the SEM image of the morphological construction of CSNPs revealed slightly spherical-like particles. Moreover, upon evaluating the SEM images, we acknowledge that while the nanoparticles are indeed isolated, discrete, and nonaggregated, they exhibit some variability in size. For CS-SQ NPs, the NPs exhibited an increase in size and different shapes due to the presence of squalene and also some aggregation. Another effective approach for elucidating the morphology of CSNPs is STEM in SEM (Figure 3B). The introduction of STEM in SEM images has led to a more expansive conceptualization than that of the SEM, particularly with regard to the nonaggregation and lower agglomeration status of CSNPs in comparison to the CS-SQ NPs. The loading of squalene on CSNPs has been demonstrated to exert an influence on the shape of the NPs, as previously observed by other research groups.[12,29] It can be concluded that squalene affects both the shape and size of chitosan nanoparticles during the synthesis process. This observation was consistent with previous findings indicating that the presence of diverse components, including curcumin, oregano essential oil, and lipids, can enhance the size of CSNPs while maintaining their spherical shape.[15,29,30,32] Also, the sizes obtained by SEM and STEM in SEM were smaller than those observed with DLS. For example, the mean size of the CSNPs and CS-SQ NPs exhibited a wide range, between 40 and 150 nm. This result was anticipated, as the particles were dried prior to observation. Conversely, DLS provided insight into the hydrodynamic diameter of the particles, and it was known that chitosan particles exhibited significant swelling in aqueous solution.[50]
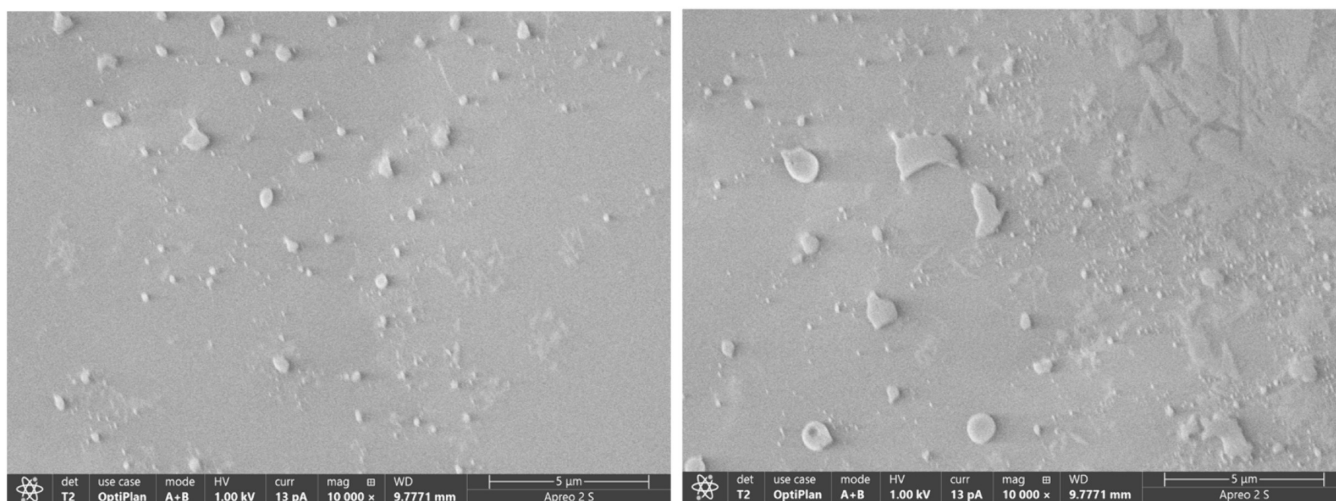
3.3. Cytotoxicity Evaluation of the Chitosan−Squalene Nanoparticles as Drug Carrier.
Currently, chitosan is widely regarded as a safe and benign polymer for the delivery of pharmaceuticals. The United States Food and Drug

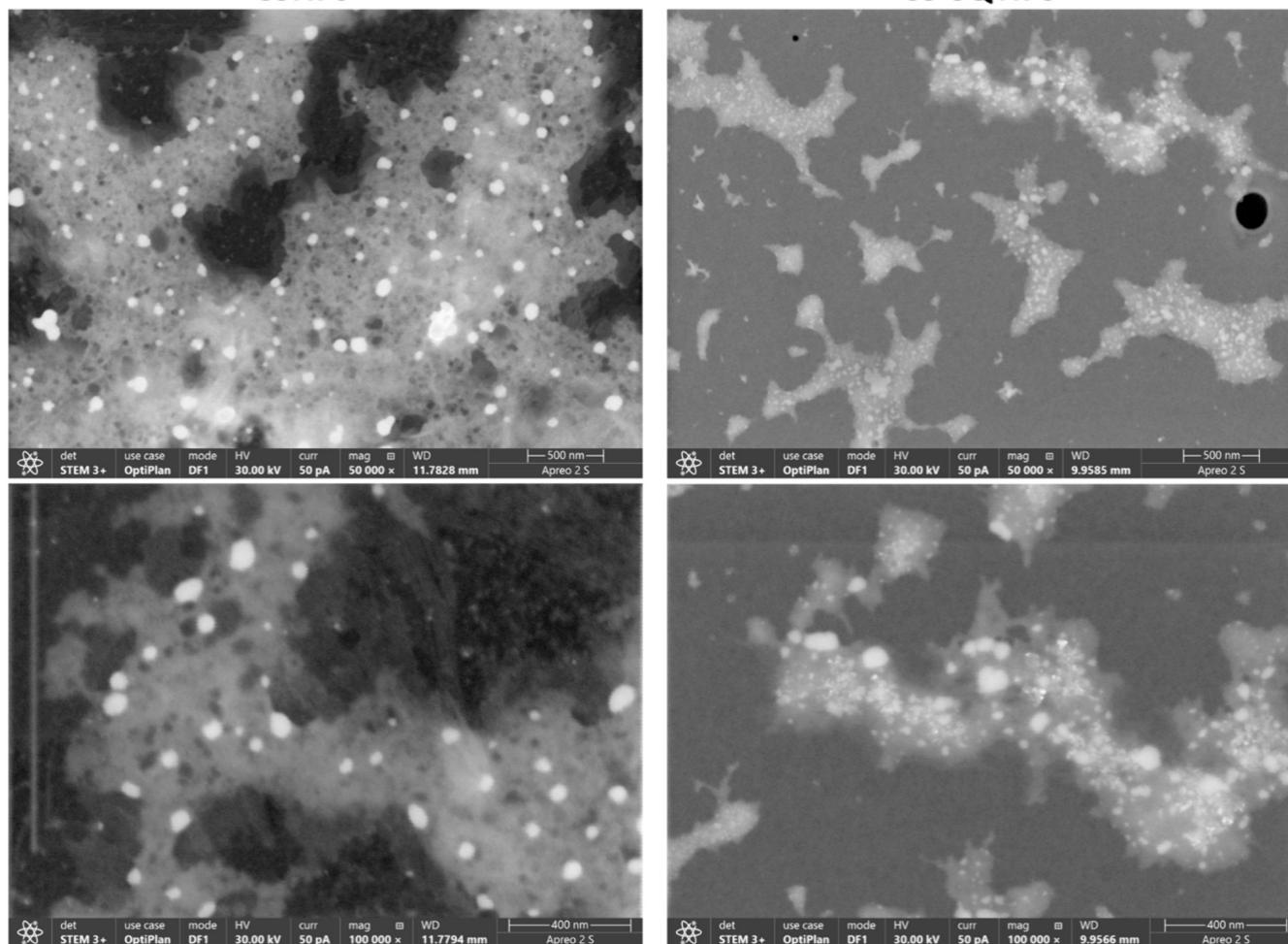**Figure 3.** (A) SEM and (B) STEM in SEM pictures of chitosan nanoparticles (CSNPs) and chitosan-squalene nanoparticles (CS-SQ NPs) (×50,000 and ×100,000).
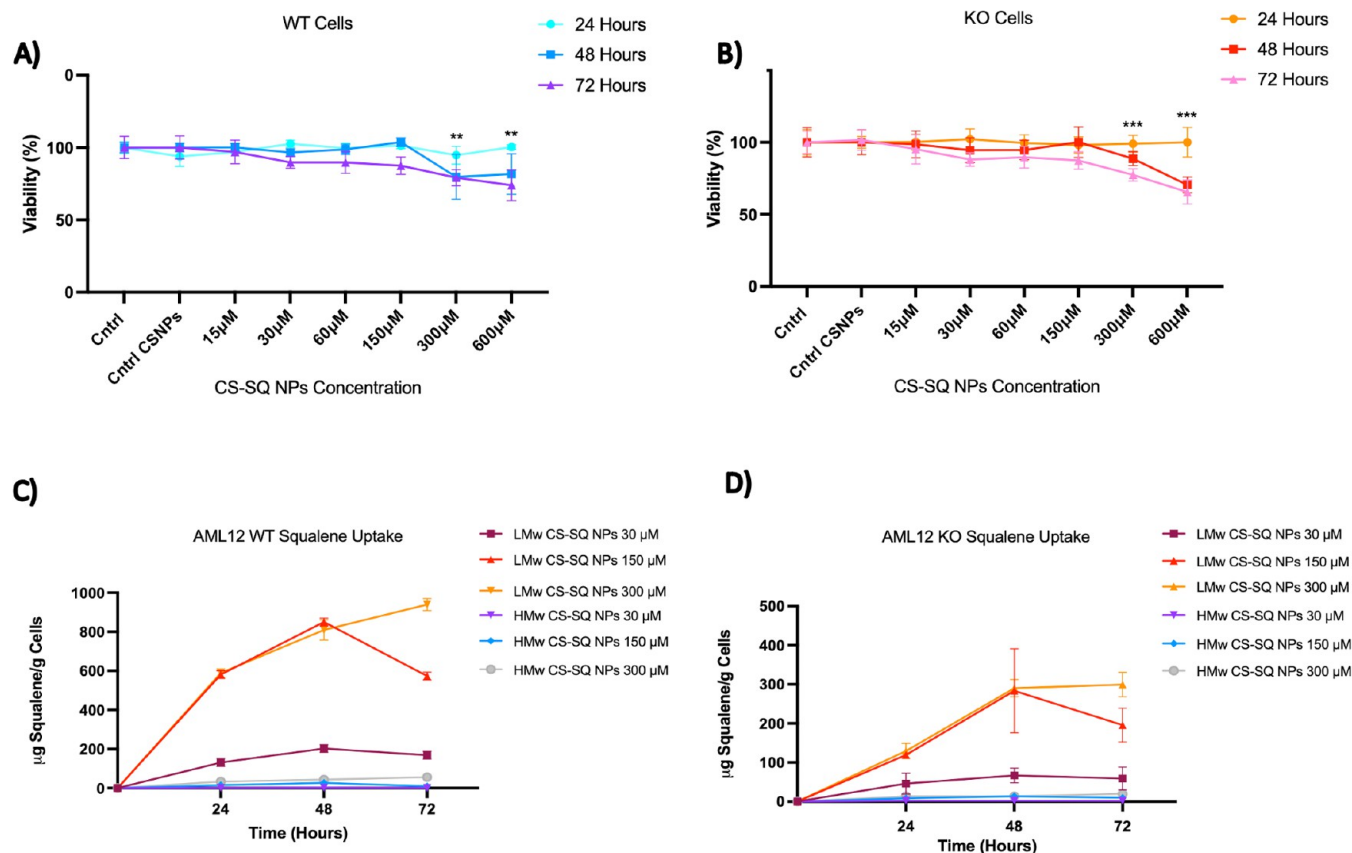
Figure 4. The viability of (A) AML12 WT cells and (B) AML12 KO cells was assessed following 24, 48, and 72 h of treatment with varying concentrations of CS-SQ NPs. A significant difference was observed between the 300 and 600 μM CS-SQ NPs and control groups. (C, D) Cellular uptake of squalene by the AML12 WT and KO cell lines, respectively. A notable enhancement in squalene uptake was observed in both WT and KO AML12 cells at 150 μM following a 48 h incubation period, as evidenced by the results of the squalene extraction. Statistical analyses were done according to Mann−Whitney's U-test: **$p < 0.01$, ***$p < 0.001$.

Administration has approved its use as a wound dressing.[51] Different results demonstrated that, due to the prolonged circulation time *in vivo* and enhanced permeability and efficacy of the drug, chitosan nanoparticles loaded with drugs were successfully concentrated in tumor tissues of mice, with a superior antitumor effect and reduced toxicity.[52] The cytotoxicities of the CS-SQ NPs and CSNPs were evaluated using MTT colorimetric assays on two distinct cell lines: AML12 WT, mouse hepatocyte cells, and AML12 KO, mouse hepatocyte cells lacking the expression of TXNDC5 protein. Both cell lines served as effective models for the investigation of hepatotoxicity associated with novel materials. In regard to the MTT assays, three-time frames and six distinct nanoparticle concentrations were selected for testing. Both cell lines demonstrated heightened sensitivity within 72 h of treatment. In fact, at 600 μM, the highest concentration tested, the cell viability was approximately 75% on the AML12 WT cell line (Figure 4A) and 65% on the AML12 KO cell line (Figure 4B). The MTT assays indicated that 24 and 48 h were safe for a maximum concentration of 150 μM on both cells, with cell viability exceeding 85%. There was no difference in cell viability between the control and CSNPs. The results of this assay indicated that neither CS-SQ NPs nor CSNPs exhibited cytotoxicity in either cell line at concentrations up to 150 μM at 24 and 48 h of treatment (Figure 4A,B). The results of this study confirmed the lack of cytotoxicity observed in previous studies involving chitosan-curcumin nanoparticles and doxor-

ubicin−chitosan polymeric micelles for targeting the liver and spleen, with a significant reduction in drug toxicity to the heart and kidney.[30,53] In contrast to toxic compounds such as sulfide, which exhibited toxicity against MCF7 and COS7 cells, chitosan has been demonstrated to be nontoxic. However, it is important to note that the concentration of chitosan may affect cell viability at high doses or for long periods of time. For example, intravenous injection of excessive amounts of chitosan has been associated with blood clotting, which could lead to adverse outcomes such as death. However, this phenomenon typically occurred at very high concentrations.[54] Consequently, in the development of CSNPs, it is important to consider the NPs concentration to minimize potential toxicity.[55]

3.4. Cellular Uptake of Squalene in AML12 Cells. A cell uptake study is an essential tool for evaluating the delivery potential of the nanoparticle system. Cellular uptake was studied with squalene extracted from hepatocytes by GC/MS. Three different LMw and HMw CS-SQ NP ratios (30, 150, and 300 μM) were tested over 24, 48, and 72 h to identify optimal conditions. As the CS-SQ NPs ratio increased, the uptake efficiency increased. Interestingly, for all CS-SQ NPs except 300 μM, the maximum cellular uptake efficiency was observed for the 150 μM ratio at 48 h, after which a decrease in uptake was observed (Figure 4C,D). This could be due to the saturation of the endocytosis pathway by the nanosystems.[56] It is our contention that saturation was reflected in the time and
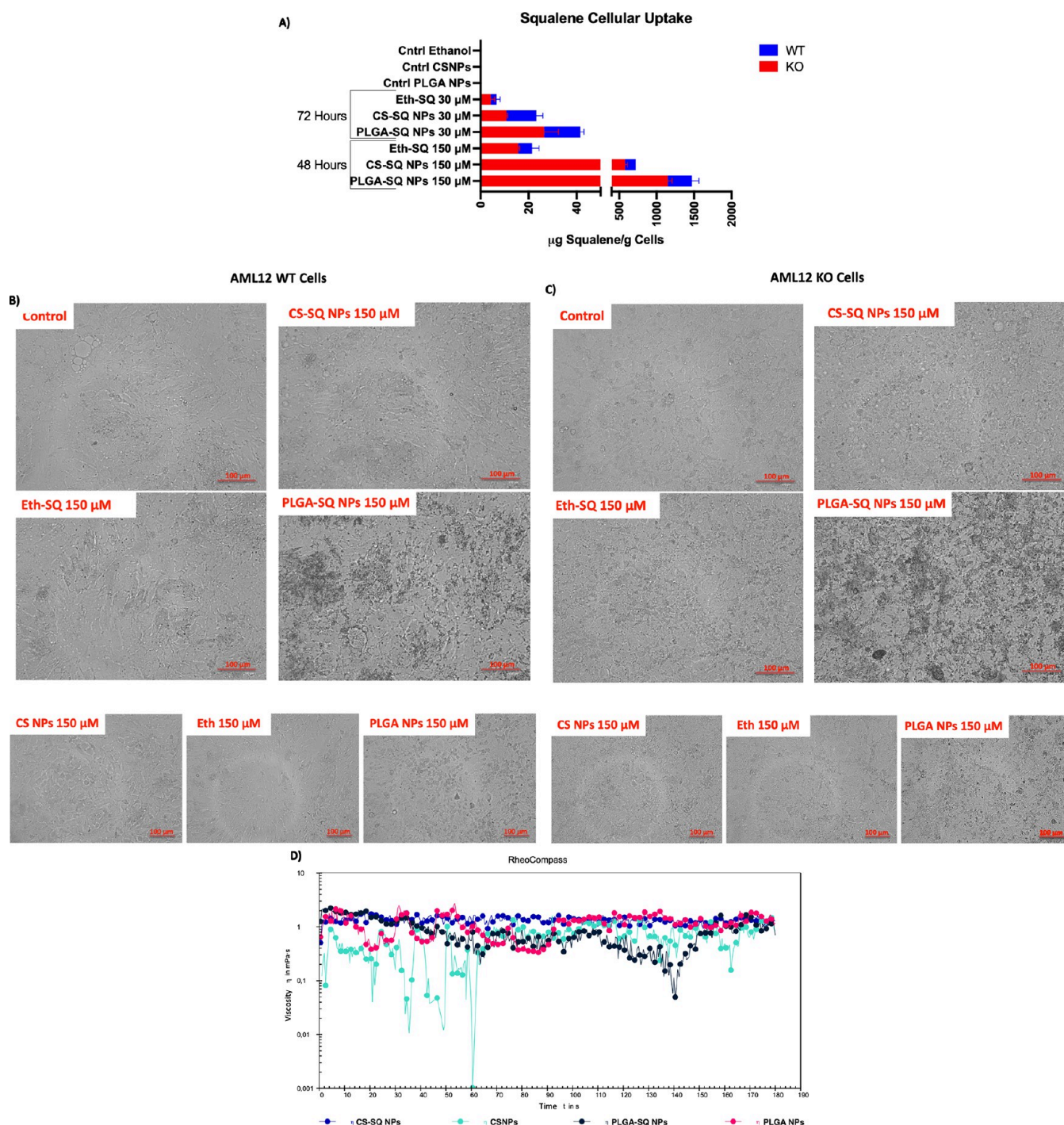
Figure 5. (A) *In vitro* cellular uptake of squalene using different carriers. WT and KO hepatic AML12 cells were incubated with 30 and 150 μM PLGA, CS-SQ NPs, and Eth-SQ for 48 and 72 h. (B, C) The effect of 48 h of exposure to different carriers at a concentration of 150 μM squalene on the morphology of AML12 WT and KO cell lines. The control group refers to untreated cells with none of the carriers. (D) Viscosity measurements of chitosan and PLGA nanoparticle solutions containing squalene compared to control nanoparticle solution.

concentration of squalene. In LMw CS-SQ NPs 150 and 300 μM, in the concentration of 150, the absorption finished after 48 h, as indicated by the decrease in cellular squalene amount at 72 h. Conversely, the cellular amount of squalene increased continuously because there were more squalene molecules to absorb. These data might be used to determine the optimal concentration for subsequent doses of charged NPs and the appropriate time interval between doses. Among the LMw and HMw CS-SQ NPs, squalene carried by LMw CS into the cells

was the most efficient in terms of the amount of squalene per gram of cells. The results indicated that the nature and molar ratios of chitosan play a significant role in their internalization process.[57] Another hypothesis regarding the In HMw CS-SQ NPs was that they are unable to be absorbed due to their larger size, which prevents them from being absorbed by cells. This indicated a loss of function of the NPs. Previous studies have shown that for a comparable number of polymer units, the use of smaller Mw chitosan on lipid nanoparticle surfaces was more

favorable for efficient cellular uptake.[58−60] Chitosan has been demonstrated to enhance the bioavailability of drugs by facilitating their absorption, which prolongs the contact time between the substrate and cell membrane.[18] Furthermore, their nanoscale dimensions facilitate the uptake of drugs through the cell membrane. This feature has been observed in A2780 ovarian cancer cells, indicating that CSNPs could deliver drugs to the perinuclear space.[61] Other studies have indicated that paclitaxel, glycol, cyclosporin A, and ovalbumin−chitosan nanoparticles had a higher cell uptake rate than the free drugs in MDA-MB-231, HeLa, RCE, and RAW264.7.[62−65] In conclusion, the results of squalene extraction indicated that there was a considerable increase in the uptake of squalene as compared to the control in 150 μM at 48 h in both WT and KO AML12 cells. The internalization and uptake of squalene-particles might be favored due to the presence of positively charged chitosan.[62] In general, the surface charge of particles is considered a crucial factor in determining their uptake by cells. For example, positively charged gold nanoparticles were preferentially captured by cells in comparison to their negatively charged counterparts.[66] CS-SQ NPs had a high positive charge, and studies have shown that cationic nanoparticles could significantly increase the endocytosis of particles.[67]

3.5. Chitosan Nanoparticles vs PLGA or Ethanol as Carriers.
The transfer of squalene into cells can be achieved through the use of various carriers, including PLGA and ethanol.[5,68] However, the optimal carrier for this purpose remains to be determined. In our experimental design, we included ethanol-squalene as a non-nanoparticle carrier to serve as a control for comparison with PLGA and CS drug delivery systems. The ethanol-squalene formulation provided a relevant baseline for the investigation of the cellular uptake and delivery efficiency of squalene when not encapsulated in NPs. Also, prior studies have evaluated the use of free CS for drug delivery, demonstrating its limited ability to encapsulate and effectively deliver hydrophobic compounds like squalene, clove essential oil, and doxorubicin without nanoparticle formulation. These studies demonstrated that CS in non-nanoparticle form provided significantly lower encapsulation efficiency and stability for hydrophobic compounds compared to nanoparticle formulations, which utilize chitosan's capacity to form stable carriers.[69−72] Previous investigations have indicated that PLGA NPs, due to their smaller size, are rapidly and efficiently taken up by cells.[73,74] In order to identify the optimal carrier for the transfer of squalene into hepatocytes, two doses of squalene (30 μM and 150 μM) were selected for comparison. These doses were carried by LMw chitosan, PLGA and ethanol,[5,68] and were administered over a 48- or 72-h exposure period. The results of squalene cellular uptake by AML12 WT and KO cells indicated that the chitosan and PLGA have higher efficiency compared to ethanol (Figure 5A). However, the PLGA-SQ NPs in both doses exhibited the highest efficiency at 48 and 72 h. These results confirmed previous findings that PLGA has superior cellular uptake compared to other polymers used for drug and gene delivery.[75] As evidenced by numerous studies, PLGA nanoparticles are highly efficient nanocarriers for the encapsulation and delivery of a diverse array of anticancer agents, including oleanolic and ursolic acids, in three distinct cell lines: HepG2, Caco-2, and Y-79.[76] For instance, PLGA-based curcumin nanoparticles have exhibited an entrapment efficiency of 77 to 85%.[77] However, the previous study conducted by our group revealed certain

limitations associated with PLGA nanoparticles. In this regard, the influence of 150, 60, 30, and 15 μM doses of squalene loaded into PLGA nanoparticles was qualitatively examined by microscopy after 72 h of incubation with AML12 cells. The 150 μM PLGA NPs caused the cell to undergo complete shrinkage due to osmotic stress. However, this shrinkage was mitigated by lowering the nanoparticle dosage. Due to the observed morphological impact of the highest doses, the 30 μM of squalene loaded in the PLGA nanoparticles was selected to carry out the subsequent studies on AML12 cells. Hence, high doses of squalene were not applicable in the PLGA carrier.[5] To ascertain the impact of CS-SQ NPs on hepatocyte morphology in the presence of high concentrations of squalene, the influence of 150 μM CS-SQ NPs, PLGA-SQ NPs, and Eth-SQ was qualitatively examined by microscopy after 48 h of incubation with WT and KO AML12 cells. Consequently, the 150 μM PLGA-SQ NPs induced a change in cell morphology (Figure 5B,C), whereas no such change was observed in CS-SQ NPs and Eth-SQ due to the presence of osmotic stress. Therefore, based on the observed morphological impact of the highest doses of squalene, chitosan was selected as the most efficient and productive carrier for high doses of squalene to conduct subsequent studies on hepatocytes.

The viscosity of polymer solution is a parameter of great interest from a technological standpoint, as highly viscous solutions present significant challenges in their management.[22] The molecular weight and viscosity of chitosan in aqueous solution also play a significant role in its biochemical and pharmacological applications.[78] The viscosity of chitosan is dependent upon the molecular weight of the polymer and the degree of deacetylation, with a reduction in viscosity observed as the molecular weight of chitosan is diminished. In fact, viscosity can be employed to ascertain the stability of the polymer in solution, as a reduction was observed during polymer storage due to polymer degradation.[79] It was evident that a certain quantity of larger nanoparticles was tolerated by the human body. In contrast to small nanoparticles, capillary blockage will occur if the particle size exceeds the diameter of the blood vessel. The gelation of the low-viscosity CS-SQ NPs and PLGA-SQ NPs dispersion in the syringe needle may occur, resulting in the immediate formation of a viscous suspension with unacceptable particle sizes. These were significant challenges for the development of squalene nanoparticle dispersions suitable for intravenous injection in clinical practice. In this context, the viscosity of the CS-SQ NPs and PLGA-SQ NPs was quantified using Pressure Cell C-PDT200. The results demonstrated that the squalene did not show any significant alterations in the viscosity of both drug delivery carriers. In addition, the viscosity of CS-SQ NPs and PLGA-SQ NPs demonstrated their ease of administration due to the formulations with lower viscosity (Figure 5D).

3.6. Squalene Protects Hepatocytes against Oxidative and Endoplasmic Reticulum Stress.
The administration of squalene has been demonstrated to induce significant alterations in hepatic proteins involved in lipid metabolism, oxidative stress, and lipoprotein secretion, as well as a reduction in hepatic triglycerides in mice.[80] Squalene's antioxidant properties are closely associated with its distinctive and stable structure, which enables it to effectively neutralize harmful free radicals.[81] Hepatic TXNDC5 is a member of the protein disulfide isomerase family, which has been associated with antisteatotic properties of squalene and regulation of ER
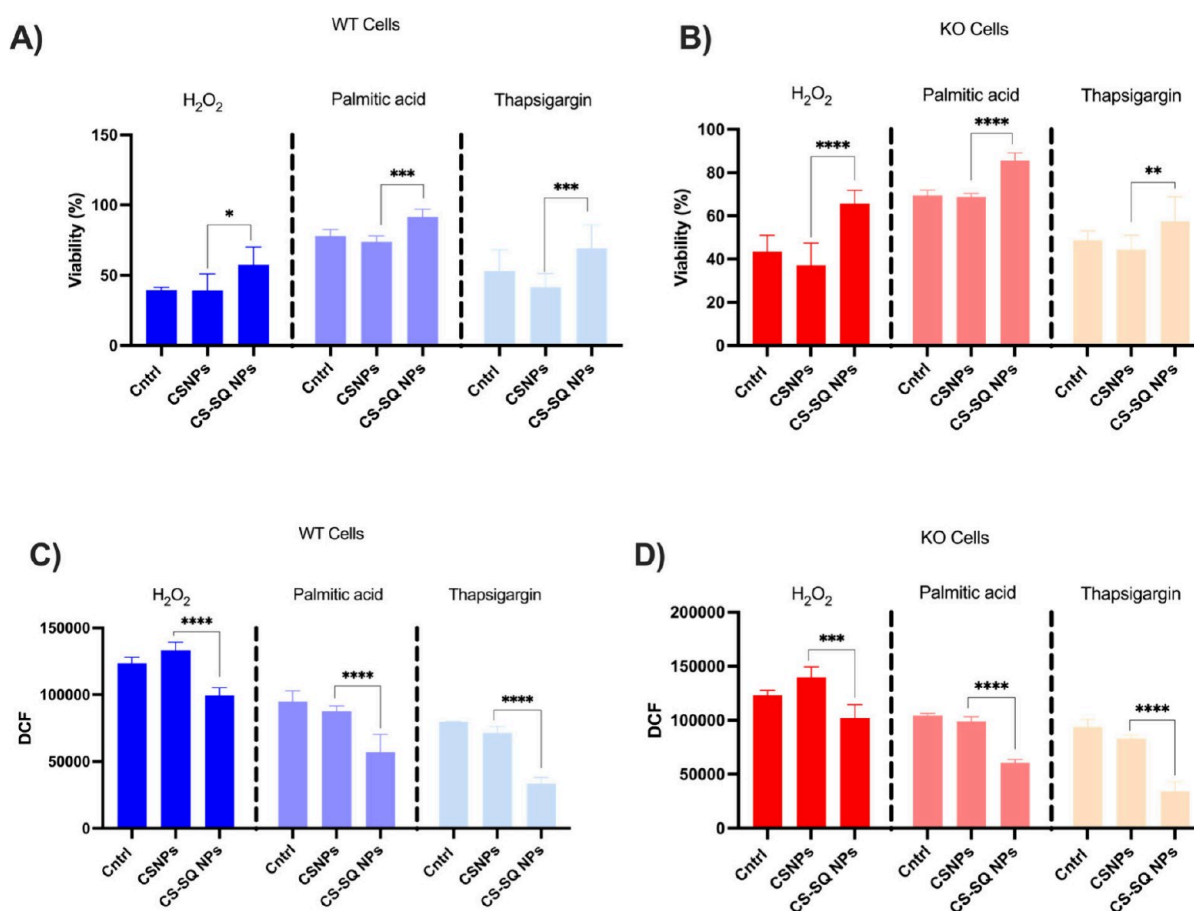
Figure 6. (A, B) The evaluation of cell viability in WT and KO AML12 hepatocytes subjected to oxidative and ER stress. Following a 48 h treatment with 150 μM of CS-SQ NPs, ER stress was induced by 12.5 nM of thapsigargin, 600 μM of palmitic acid, and oxidative stress was induced by 8 mM of H_2O_2 for 24 h. (C, D) Assessment of ROS production in AML12 WT and KO cells, respectively. Following the treatment of cells with 150 μM of CS-SQ NPs for 48 h, ROS was measured in oxidative and ER stress circumstances induced by 8 mM of H_2O_2, 600 μM of palmitic acid, and 12.5 nM of thapsigargin for 24 h. Statistical analyses were conducted according to two-way ANOVA: $**p < 0.01$, $***p < 0.001$, $***p < 0.001$, $****p < 0.0001$.

stress.[82,83] Furthermore, TXNDC5 has demonstrated potential for the diagnosis and treatment of various diseases by reducing oxidative stress and levels of inflammatory cytokines. Consequently, TXNDC5 acts as a protective agent, safeguarding cells against oxidative and ER stress.[13] AML12 cells were incubated with 150 μM of CS-SQ NPs for 48 h to assess the induction of intracellular ROS and viability by squalene. Following exposure to squalene, the cells were treated with H_2O_2 as an oxidative stress inducer, palmitic acid and thapsigargin as moderate and harsh ER stressors for 24 h. The CSNPs did not produce a notable alteration in cell viability when compared to the control group, as determined by the MTT assay. CS-SQ NPs demonstrated the capacity to significantly enhance the viability of both cell lines (Figure 6A,B). Viability enhancement was calculated in the different stressors that were tested, and the results demonstrated that the squalene delivered from chitosan nanoparticles increased the viability of the WT hepatocyte cells and KO cells by 18 and 25% in oxidative stress, respectively, and 21 and 15% in ER stress, respectively. To ascertain whether 150 μM of squalene-loaded NPs could effectively provide protection against oxidative and ER stress, we initially developed an in vitro model of them. The comparison of the control group and the CSNPs demonstrates that chitosan nanoparticles did not induce a significant ROS in both cell lines. As illustrated in

Figure 6C, WT cells treated with CS-SQ NPs exhibited a significant reduction in ROS production compared with the CS group in all stress conditions. This data was also observed in KO samples (Figure 6D), although previous data from our group indicated that squalene protection was absent in cells lacking TXNDC5 when exposed to 30 μM of squalene in an oxidative stress context.[5] The protective effects of squalene against oxidative destruction have been formally documented in rodents and multiple cell lines, including murine macrophages, human monocytes, and mammary epithelial cells.[84] Previous studies have demonstrated that inhibiting TXNDC5 expression via knockdown induced ROS and ER stress in pancreatic cancer cells. Conversely, increasing TXNDC5 expression in lipid endothelial cells effectively reduced ROS production and protects cells.[85,86] Additionally, the overexpression of TXNDC5 resulted in reduced sensitivity to ER stress when exposed to tunicamycin and thapsigargin. However, TXNDC5 knockout human prostate adenocarcinoma cells exhibited a loss of the ability to upregulate protein disulfide isomerase following tunicamycin-induced ER stress.[87] Overall, the results demonstrated that TXNDC5 could modulate ROS production in oxidative stress, contingent on the optimal dose of squalene, and enhanced the efficacy of squalene in AML12 cell viability and functioned as an oxidative stress-induced survival factor that regulated ROS/ER stress

signaling, thereby enabling AML12 cells to persist under oxidative stress.

4. CONCLUSIONS

The present study demonstrates that low molecular weight chitosan nanoparticles, which form a spherical shape, are an effective encapsulation agent for squalene based on GC-MS measurement and semiquantitative FTIR analysis. The results demonstrated that squalene-loaded chitosan nanoparticles did not exhibit any cytotoxicity to hepatocytes up to 150 μM and exhibited efficient cellular uptake within 48 h. In comparison to PLGA and ethanol, the chitosan nanoparticles were identified as the most efficient and productive carriers for high doses of squalene and PLGA for lower doses of squalene, thus justifying further investigation in hepatocytes. The cell viability of WT and KO AML12 cells was increased in the presence of squalene under oxidative and endoplasmic reticulum stress conditions induced by palmitic acid and thapsigargin. Furthermore, squalene-based chitosan nanoparticles effectively reduced ROS levels in mouse hepatocytes. Chitosan nanoparticles demonstrated the potential to overcome the limitations of PLGA drug carriers, suggesting that the proper dose of squalene can modulate ROS production in oxidative stress, independent of TXNDC5.

■ ASSOCIATED CONTENT

Data Availability Statement

Data are contained within the article and Supporting Information.

ⓢ Supporting Information

The Supporting Information is available free of charge at https://pubs.acs.org/doi/10.1021/acsomega.4c08258.

Figure S1 showing characterization of AML12 cell lines (PDF)

■ AUTHOR INFORMATION

Corresponding Authors

Jesús Osada − *Departamento de Bioquímica y Biología Molecular y Celular, Facultad de Veterinaria, Instituto de Investigación Sanitaria de Aragón, Universidad de Zaragoza, E-50013 Zaragoza, Spain; Instituto Agroalimentario de Aragón, CITA-Universidad de Zaragoza, E-50013 Zaragoza, Spain; Centro de Investigación Biomédica en Red de Fisiopatología de la Obesidad y Nutrición (CIBEROBN), Instituto de Salud Carlos III, E-28029 Madrid, Spain; Departamento de Farmacología, Fisiología, Medicina Legal y Forense, Facultad de Veterinaria, Instituto de Investigación Sanitaria de Aragón-Universidad de Zaragoza, E-50013 Zaragoza, Spain;* Phone: +34-976-761-644; Email: josada@unizar.es; Fax: +34-976-761-612

Susana C. M. Fernandes − *Institute of Analytical Sciences and Physico-Chemistry for Environment and Materials (IPREM), E2S UPPA, CNRS, Université de Pau et des Pays de l'Adour, 64 012 Pau, France; MANTA—Marine Materials Research Group, Universite de Pau et des Pays de l'Adour, 64 053 Pau, France;* ⓘ orcid.org/0000-0002-1295-5010; Phone: +33 (0) 5 40 17 50 15; Email: susana.fernandes@univ-pau.fr

Authors

Seyed Hesamoddin Bidooki − *Departamento de Bioquímica y Biología Molecular y Celular, Facultad de Veterinaria, Instituto de Investigación Sanitaria de Aragón, Universidad de Zaragoza, E-50013 Zaragoza, Spain; Institute of Analytical Sciences and Physico-Chemistry for Environment and Materials (IPREM), E2S UPPA, CNRS, Université de Pau et des Pays de l'Adour, 64 012 Pau, France; MANTA—Marine Materials Research Group, Universite de Pau et des Pays de l'Adour, 64 053 Pau, France;* ⓘ orcid.org/0000-0002-5612-5000

Lea Spitzer − *Institute of Analytical Sciences and Physico-Chemistry for Environment and Materials (IPREM), E2S UPPA, CNRS, Université de Pau et des Pays de l'Adour, 64 012 Pau, France; MANTA—Marine Materials Research Group, Universite de Pau et des Pays de l'Adour, 64 053 Pau, France*

Arnaud Petitpas − *Institute of Analytical Sciences and Physico-Chemistry for Environment and Materials (IPREM), E2S UPPA, CNRS, Université de Pau et des Pays de l'Adour, 64 012 Pau, France; MANTA—Marine Materials Research Group, Universite de Pau et des Pays de l'Adour, 64 053 Pau, France*

Javier Sánchez-Marco − *Departamento de Bioquímica y Biología Molecular y Celular, Facultad de Veterinaria, Instituto de Investigación Sanitaria de Aragón, Universidad de Zaragoza, E-50013 Zaragoza, Spain*

Roberto Martínez-Beamonte − *Departamento de Bioquímica y Biología Molecular y Celular, Facultad de Veterinaria, Instituto de Investigación Sanitaria de Aragón, Universidad de Zaragoza, E-50013 Zaragoza, Spain; Instituto Agroalimentario de Aragón, CITA-Universidad de Zaragoza, E-50013 Zaragoza, Spain; Centro de Investigación Biomédica en Red de Fisiopatología de la Obesidad y Nutrición (CIBEROBN), Instituto de Salud Carlos III, E-28029 Madrid, Spain*

Roberto Lasheras − *Laboratorio Agroambiental, Servicio de Seguridad Agroalimentaria de la Dirección General de Alimentación y Fomento Agroalimentario, Gobierno de Aragón, E-50192 Zaragoza, Spain*

Virginie Pellerin − *Institute of Analytical Sciences and Physico-Chemistry for Environment and Materials (IPREM), E2S UPPA, CNRS, Université de Pau et des Pays de l'Adour, 64 012 Pau, France*

María J. Rodríguez-Yoldi − *Instituto Agroalimentario de Aragón, CITA-Universidad de Zaragoza, E-50013 Zaragoza, Spain; Centro de Investigación Biomédica en Red de Fisiopatología de la Obesidad y Nutrición (CIBEROBN), Instituto de Salud Carlos III, E-28029 Madrid, Spain; Departamento de Farmacología, Fisiología, Medicina Legal y Forense, Facultad de Veterinaria, Instituto de Investigación Sanitaria de Aragón-Universidad de Zaragoza, E-50013 Zaragoza, Spain*

María Angeles Navarro − *Departamento de Bioquímica y Biología Molecular y Celular, Facultad de Veterinaria, Instituto de Investigación Sanitaria de Aragón, Universidad de Zaragoza, E-50013 Zaragoza, Spain; Instituto Agroalimentario de Aragón, CITA-Universidad de Zaragoza, E-50013 Zaragoza, Spain; Centro de Investigación Biomédica en Red de Fisiopatología de la Obesidad y Nutrición (CIBEROBN), Instituto de Salud Carlos III, E-28029 Madrid, Spain*

Complete contact information is available at:
https://pubs.acs.org/10.1021/acsomega.4c08258

Author Contributions

Conceptualization: S.H.B., L.S., A.P., V.P., J.S.-M., R.M.-B., R.L., M.A.N., M.J.R.-Y., J.O., and S.C.M.F. Methodology: S.H.B., L.S., A.P., V.P., J.S.-M., R.M.-B., and R.L. Software: S.H.B., A.P., and V.P. Validation: S.H.B. Formal analysis: S.H.B., L.S., A.P., V.P., J.S.-M., R.M.-B., and R.L. Investigation: S.H.B., J.O., and S.C.M.F. Resources: M.J.R.-Y., J.O., and S.C.M.F. Data curation: M.A.N., M.J.R.-Y., J.O. and S.C.M.F. Writing—original draft preparation: S.H.B. Writing—review and editing: S.H.B., L.S., A.P., V.P., J.S.-M., R.M.-B., R.L., M.A.N., M.J.R.-Y., J.O., and S.C.M.F. Visualization: S.H.B., A.P., V.P. Supervision: M.A.N., J.O., and S.C.M.F. Project administration: M.J.R.-Y., J.O., and S.C.M.F. Funding acquisition: M.J.R.-Y., J.O., and S.C.M.F. All authors have read and agreed to the published version of the manuscript.

Notes

The authors declare no competing financial interest.

■ REFERENCES

(1) Hatchwell, L.; Harney, D. J.; Cielesh, M.; Young, K.; Koay, Y. C.; O'Sullivan, J. F.; Larance, M. Multi-omics analysis of the intermittent fasting response in mice identifies an unexpected role for HNF4α. *Cell Reports* **2020**, *30* (10), 3566–3582.

(2) Herrera-Marcos, L. V.; Martínez-Beamonte, R.; Macías-Herranz, M.; Arnal, C.; Barranquero, C.; Puente-Lanzarote, J. J.; Gascón, S.; Herrero-Continente, T.; Gonzalo-Romeo, G.; Alastrué-Vera, V.; et al. Hepatic galectin-3 is associated with lipid droplet area in non-alcoholic steatohepatitis in a new swine model. *Sci. Rep.* **2022**, *12* (1), 1024.

(3) Tu, L. N.; Showalter, M. R.; Cajka, T.; Fan, S.; Pillai, V. V.; Fiehn, O.; Selvaraj, V. Metabolomic characteristics of cholesterol-induced non-obese nonalcoholic fatty liver disease in mice. *Sci. Rep.* **2017**, *7* (1), 6120.

(4) Guasch-Ferré, M.; Willett, W. The Mediterranean diet and health: A comprehensive overview. *Journal of internal medicine* **2021**, *290* (3), 549–566.

(5) Bidooki, S. H.; Alejo, T.; Sánchez-Marco, J.; Martínez-Beamonte, R.; Abuobeid, R.; Burillo, J. C.; Lasheras, R.; Sebastian, V.; Rodríguez-Yoldi, M. J.; Arruebo, M.; Osada, J. Squalene loaded nanoparticles effectively protect hepatic AML12 cell lines against oxidative and endoplasmic reticulum stress in a TXNDC5-dependent way. *Antioxidants* **2022**, *11* (3), 581.

(6) Guasch-Ferré, M.; Li, Y.; Willett, W. C.; Sun, Q.; Sampson, L.; Salas-Salvadó, J.; Martínez-González, M. A.; Stampfer, M. J.; Hu, F. B. Consumption of olive oil and risk of total and cause-specific mortality among US adults. *Journal of the American College of Cardiology* **2022**, *79* (2), 101–112.

(7) Martínez-Beamonte, R.; Sánchez-Marco, J.; Felices, M. J.; Barranquero, C.; Gascón, S.; Arnal, C.; Burillo, J. C.; Lasheras, R.; Busto, R.; Lasunción, M. A.; et al. Dietary squalene modifies plasma lipoproteins and hepatic cholesterol metabolism in rabbits. *Food Funct.* **2021**, *12* (17), 8141–8153.

(8) Gabás-Rivera, C.; Barranquero, C.; Martínez-Beamonte, R.; Navarro, M. A.; Surra, J. C.; Osada, J. Dietary squalene increases high density lipoprotein-cholesterol and paraoxonase 1 and decreases oxidative stress in mice. *PloS one* **2014**, *9* (8), No. e104224.

(9) Spanova, M.; Daum, G. Squalene-biochemistry, molecular biology, process biotechnology, and applications. *European journal of lipid science and technology* **2011**, *113* (11), 1299–1320.

(10) Lou-Bonafonte, J. M.; Martínez-Beamonte, R.; Sanclemente, T.; Surra, J. C.; Herrera-Marcos, L. V.; Sanchez-Marco, J.; Arnal, C.; Osada, J. Current insights into the biological action of squalene. *Mol. Nutr. Food Res.* **2018**, *62* (15), 1800136.

(11) Reddy, L. H.; Couvreur, P. Squalene: A natural triterpene for use in disease management and therapy. *Advanced drug delivery reviews* **2009**, *61* (15), 1412–1426.

(12) Kumar, L. R.; Chatterjee, N.; Tejpal, C.; Vishnu, K.; Anas, K.; Asha, K.; Anandan, R.; Mathew, S. Evaluation of chitosan as a wall material for microencapsulation of squalene by spray drying: Characterization and oxidative stability studies. *Int. J. Biol. Macromol.* **2017**, *104*, 1986–1995.

(13) Bidooki, S. H.; Navarro, M. A.; Fernandes, S. C. M.; Osada, J. Thioredoxin Domain Containing 5 (TXNDC5): Friend or Foe? *Current Issues in Molecular Biology* **2024**, *46* (4), 3134–3163.

(14) Wang, J. J.; Zeng, Z. W.; Xiao, R. Z.; Xie, T.; Zhou, G. L.; Zhan, X. R.; Wang, S. L. Recent advances of chitosan nanoparticles as drug carriers. *Int. J. Nanomed.* **2011**, 765–774.

(15) Khan, M. M.; Madni, A.; Torchilin, V.; Filipczak, N.; Pan, J.; Tahir, N.; Shah, H. Lipid-chitosan hybrid nanoparticles for controlled delivery of cisplatin. *Drug delivery* **2019**, *26* (1), 765–772.

(16) Lekshmi, R. K.; Rahima, M.; Chatterjee, N.; Tejpal, C.; Anas, K.; Vishnu, K.; Sarika, K.; Asha, K.; Anandan, R.; Suseela, M. Chitosan-Whey protein as efficient delivery system for squalene: Characterization and functional food application. *Int. J. Biol. Macromol.* **2019**, *135*, 855–863.

(17) Fernández-Marín, R.; Fernandes, S. C. M.; Sánchez, M. Á. A.; Labidi, J. Halochromic and antioxidant capacity of smart films of chitosan/chitin nanocrystals with curcuma oil and anthocyanins. *Food Hydrocolloids* **2022**, *123*, 107119.

(18) Tiyaboonchai, W. Chitosan nanoparticles: a promising system for drug delivery. *Naresuan University Journal: Science and Technology (NUJST)* **2003**, *11* (3), 51–66.

(19) Rampino, A.; Borgogna, M.; Blasi, P.; Bellich, B.; Cesàro, A. Chitosan nanoparticles: Preparation, size evolution and stability. *International journal of pharmaceutics* **2013**, *455* (1–2), 219–228.

(20) Salaberria, A. M.; Diaz, R. H.; Labidi, J.; Fernandes, S. C. M. Preparing valuable renewable nanocomposite films based exclusively on oceanic biomass-Chitin nanofillers and chitosan. *React. Funct. Polym.* **2015**, *89*, 31–39.

(21) Claverie, M.; McReynolds, C.; Petitpas, A.; Thomas, M.; Fernandes, S. C. M. Marine-derived polymeric materials and biomimetics: An overview. *Polymers* **2020**, *12* (5), 1002.

(22) Aranaz, I.; Alcántara, A. R.; Civera, M. C.; Arias, C.; Elorza, B.; Heras Caballero, A.; Acosta, N. Chitosan: An overview of its properties and applications. *Polymers* **2021**, *13* (19), 3256.

(23) Bekmukhametova, A.; Uddin, M. M. N.; Houang, J.; Malladi, C.; George, L.; Wuhrer, R.; Barman, S. K.; Wu, M. J.; Mawad, D.; Lauto, A. Fabrication and characterization of chitosan nanoparticles using the coffee-ring effect for photodynamic therapy. *Lasers in Surgery and Medicine* **2022**, *54* (5), 758–766.

(24) Gan, Q.; Wang, T. Chitosan nanoparticle as protein delivery carrier—systematic examination of fabrication conditions for efficient loading and release. *Colloids Surf., B* **2007**, *59* (1), 24–34.

(25) Cardoso, M. J.; Costa, R. R.; Mano, J. F. Marine origin polysaccharides in drug delivery systems. *Marine drugs* **2016**, *14* (2), 34.

(26) Pinto, R. J.; Fernandes, S. C. M.; Freire, C. S.; Sadocco, P.; Causio, J.; Neto, C. P.; Trindade, T. Antibacterial activity of optically transparent nanocomposite films based on chitosan or its derivatives and silver nanoparticles. *Carbohydr. Res.* 2012, *348*, 77–83.

(27) Zubillaga, V. n.; Salaberria, A. M.; Palomares, T.; Alonso-Varona, A.; Kootala, S.; Labidi, J.; Fernandes, S. C. M. Chitin nanoforms provide mechanical and topological cues to support growth of human adipose stem cells in chitosan matrices. *Biomacromolecules* 2018, *19* (7), 3000–3012.

(28) Divya, K.; Jisha, M. Chitosan nanoparticles preparation and applications. *Environmental chemistry letters* 2018, *16*, 101–112.

(29) Lepeltier, E.; Loretz, B.; Desmaële, D.; Zapp, J.; Herrmann, J.; Couvreur, P.; Lehr, C.-M. Squalenoylation of chitosan: a platform for drug delivery? *Biomacromolecules* 2015, *16* (9), 2930–2939.

(30) Ma, S.; Moser, D.; Han, F.; Leonhard, M.; Schneider-Stickler, B.; Tan, Y. Preparation and antibiofilm studies of curcumin loaded chitosan nanoparticles against polymicrobial biofilms of Candida albicans and Staphylococcus aureus. *Carbohydr. Polym.* 2020, *241*, 116254.

(31) Tezgel, Ö.; Szarpak-Jankowska, A.; Arnould, A.; Auzély-Velty, R.; Texier, I. Chitosan-lipid nanoparticles (CS-LNPs): Application to siRNA delivery. *J. Colloid Interface Sci.* 2018, *510*, 45–56.

(32) Hosseini, S. F.; Zandi, M.; Rezaei, M.; Farahmandghavi, F. Two-step method for encapsulation of oregano essential oil in chitosan nanoparticles: Preparation, characterization and in vitro release study. *Carbohydr. Polym.* 2013, *95* (1), 50–56.

(33) Kumar, L.; Verma, S.; Singh, K.; Prasad, D. N.; Jain, A. K. Ethanol based vesicular carriers in transdermal drug delivery: nanoethosomes and transethosomes in focus. *NanoWorld J.* 2016, *2*, 41.

(34) Chu, B.-S.; Ichikawa, S.; Kanafusa, S.; Nakajima, M. Preparation and characterization of β-carotene nanodispersions prepared by solvent displacement technique. *Journal of agricultural and food chemistry* 2007, *55* (16), 6754–6760.

(35) Martínez-Beamonte, R.; Alda, O.; Sanclemente, T.; Felices, M. J.; Escusol, S.; Arnal, C.; Herrera-Marcos, L. V.; Gascón, S.; Surra, J. C.; Osada, J.; Rodriguez-Yoldi, M. J. Hepatic subcellular distribution of squalene changes according to the experimental setting. *J. Physiol. Biochem.* 2018, *74*, 531–538.

(36) Bidooki, S. H.; Barranquero, C.; Sánchez-Marco, J.; Martínez-Beamonte, R.; Rodríguez-Yoldi, M. J.; Navarro, M. A.; Fernandes, S. C. M.; Osada, J. TXNDC5 Plays a Crucial Role in Regulating Endoplasmic Reticulum Activity through Different ER Stress Signaling Pathways in Hepatic Cells. *International Journal of Molecular Sciences* 2024, *25* (13), 7128.

(37) Zhao, L.-M.; Shi, L.-E.; Zhang, Z.-L.; Chen, J.-M.; Shi, D.-D.; Yang, J.; Tang, Z.-X. Preparation and application of chitosan nanoparticles and nanofibers. *Brazilian Journal of Chemical Engineering* 2011, *28*, 353–362.

(38) Qi, L.; Xu, Z.; Jiang, X.; Hu, C.; Zou, X. Preparation and antibacterial activity of chitosan nanoparticles. *Carbohydrate research* 2004, *339* (16), 2693–2700.

(39) De Campos, A. M.; Sánchez, A.; Alonso, M. a. J. Chitosan nanoparticles: a new vehicle for the improvement of the delivery of drugs to the ocular surface. Application to cyclosporin A. *International journal of pharmaceutics* 2001, *224* (1–2), 159–168.

(40) Csaba, N.; Köping-Höggård, M.; Alonso, M. J. Ionically crosslinked chitosan/tripolyphosphate nanoparticles for oligonucleotide and plasmid DNA delivery. *International journal of pharmaceutics* 2009, *382* (1–2), 205–214.

(41) Luangtana-anan, M.; Opanasopit, P.; Ngawhirunpat, T.; Nunthanid, J.; Sriamornsak, P.; Limmatvapirat, S.; Lim, L. Y. Effect of chitosan salts and molecular weight on a nanoparticulate carrier for therapeutic protein. *Pharm. Dev. Technol.* 2005, *10* (2), 189–196.

(42) Mohammadpour Dounighi, N.; Eskandari, R.; Avadi, M. R.; Zolfagharian, H.; Mir Mohammad Sadeghi, A.; Rezayat, M. Preparation and in vitro characterization of chitosan nanoparticles containing Mesobuthus eupeus scorpion venom as an antigen delivery system. *Journal of Venomous Animals and Toxins Including Tropical Diseases* 2012, *18*, 44–52.

(43) Gan, Q.; Wang, T.; Cochrane, C.; McCarron, P. Modulation of surface charge, particle size and morphological properties of chitosan-TPP nanoparticles intended for gene delivery. *Colloids Surf., B* 2005, *44* (2–3), 65–73.

(44) Souza, M. P.; Vaz, A. F.; Correia, M. T.; Cerqueira, M. A.; Vicente, A. A.; Carneiro-da-Cunha, M. G. Quercetin-loaded lecithin/chitosan nanoparticles for functional food applications. *Food and bioprocess technology* 2014, *7*, 1149–1159.

(45) Cho, K.; Wang, X.; Nie, S.; Chen, Z.; Shin, D. M. Therapeutic nanoparticles for drug delivery in cancer. *Clinical cancer research* 2008, *14* (5), 1310–1316.

(46) Keawchaoon, L.; Yoksan, R. Preparation, characterization and in vitro release study of carvacrol-loaded chitosan nanoparticles. *Colloids Surf., B* 2011, *84* (1), 163–171.

(47) Ceruti, M.; Viola, F.; Balliano, G.; Milla, P.; Roma, G.; Grossi, G.; Rocco, F. Synthesis of (E)-and (Z)-29-methylidyne-2, 3-oxidosqualene derivatives as inhibitors of liver and yeast oxidosqualene cyclase. *Journal of the Chemical Society, Perkin Transactions 1* 2002, No. 12, 1477–1486.

(48) Liu, G.; Gan, J.; Chen, A.; Liu, Q.; Zhao, X. Synthesis and characterization of an amphiphilic chitosan bearing octyl and methoxy polyethylene. *Nat. Sci.* 2010, *2* (07), 707.

(49) Huang, Z.; Wang, H.; Gao, C.; Shen, H.; Fa, X. e. Drug loaded gold nano-particulates for therapeutics of myocardial infarction in rat model. *Journal of Biomaterials and Tissue Engineering* 2018, *8* (2), 197–205.

(50) de Moura, M. R.; Aouada, F. A.; Mattoso, L. H. Preparation of chitosan nanoparticles using methacrylic acid. *J. Colloid Interface Sci.* 2008, *321* (2), 477–483.

(51) Wedmore, I.; McManus, J. G.; Pusateri, A. E.; Holcomb, J. B. A special report on the chitosan-based hemostatic dressing: experience in current combat operations. *Journal of Trauma and Acute Care Surgery* 2006, *60* (3), 655–658.

(52) Kim, J.-H.; Kim, Y.-S.; Park, K.; Lee, S.; Nam, H. Y.; Min, K. H.; Jo, H. G.; Park, J. H.; Choi, K.; Jeong, S. Y.; et al. Antitumor efficacy of cisplatin-loaded glycol chitosan nanoparticles in tumor-bearing mice. *J. Controlled Release* 2008, *127* (1), 41–49.

(53) Xu, X.; Zhou, J.; Li, L.; Zhang, Y.; Huo, M.; Wang, X.; Lü, L. Preparation of doxorubicin-loaded chitosan polymeric micelle and study on its tissue biodistribution in mice. *Yao Xue Xue Bao* 2008, *43* (7), 743–748.

(54) Kean, T.; Thanou, M. Biodegradation, biodistribution and toxicity of chitosan. *Advanced drug delivery reviews* 2010, *62* (1), 3–11.

(55) Ghormade, V.; Deshpande, M. V.; Paknikar, K. M. Perspectives for nano-biotechnology enabled protection and nutrition of plants. *Biotechnology advances* 2011, *29* (6), 792–803.

(56) Sato, T.; Ishii, T.; Okahata, Y. In vitro gene delivery mediated by chitosan. Effect of pH, serum, and molecular mass of chitosan on the transfection efficiency. *Biomaterials* 2001, *22* (15), 2075–2080.

(57) Nguyen, J.; Szoka, F. C. Nucleic acid delivery: the missing pieces of the puzzle? *Accounts of chemical research* 2012, *45* (7), 1153–1162.

(58) Ragelle, H.; Vandermeulen, G.; Préat, V. Chitosan-based siRNA delivery systems. *J. Controlled Release* 2013, *172* (1), 207–218.

(59) Dash, M.; Chiellini, F.; Ottenbrite, R. M.; Chiellini, E. Chitosan—A versatile semi-synthetic polymer in biomedical applications. *Prog. Polym. Sci.* 2011, *36* (8), 981–1014.

(60) Ying, X.-Y.; Cui, D.; Yu, L.; Du, Y.-Z. Solid lipid nanoparticles modified with chitosan oligosaccharides for the controlled release of doxorubicin. *Carbohydr. Polym.* 2011, *84* (4), 1357–1364.

(61) Yue, Z.-G.; Wei, W.; Lv, P.-P.; Yue, H.; Wang, L.-Y.; Su, Z.-G.; Ma, G.-H. Surface charge affects cellular uptake and intracellular trafficking of chitosan-based nanoparticles. *Biomacromolecules* 2011, *12* (7), 2440–2446.

(62) Gokce, E. H.; Sandri, G.; Bonferoni, M. C.; Rossi, S.; Ferrari, F.; Güneri, T.; Caramella, C. Cyclosporine A loaded SLNs: evaluation

of cellular uptake and corneal cytotoxicity. *International journal of pharmaceutics* **2008**, *364* (1), 76−86.

(63) Nam, H. Y.; Kwon, S. M.; Chung, H.; Lee, S.-Y.; Kwon, S.-H.; Jeon, H.; Kim, Y.; Park, J. H.; Kim, J.; Her, S.; et al. Cellular uptake mechanism and intracellular fate of hydrophobically modified glycol chitosan nanoparticles. *J. Controlled Release* **2009**, *135* (3), 259−267.

(64) Trickler, W.; Nagvekar, A.; Dash, A. K. A novel nanoparticle formulation for sustained paclitaxel delivery. *AAPS PharmSciTech* **2008**, *9*, 486−493.

(65) Gao, X.; Gong, J.; Cai, Y.; Wang, J.; Wen, J.; Peng, L.; Ji, H.; Jiang, S.; Guo, D. Chitosan modified squalene nanostructured lipid carriers as a promising adjuvant for freeze-dried ovalbumin vaccine. *Int. J. Biol. Macromol.* **2021**, *188*, 855−862.

(66) Boisselier, E.; Astruc, D. Gold nanoparticles in nanomedicine: preparations, imaging, diagnostics, therapies and toxicity. *Chem. Soc. Rev.* **2009**, *38* (6), 1759−1782.

(67) Yue, H.; Wei, W.; Yue, Z.; Lv, P.; Wang, L.; Ma, G.; Su, Z. Particle size affects the cellular response in macrophages. *European journal of pharmaceutical sciences* **2010**, *41* (5), 650−657.

(68) Abuobeid, R.; Sánchez-Marco, J.; Felices, M. J.; Arnal, C.; Burillo, J. C.; Lasheras, R.; Busto, R.; Lasunción, M. A.; Rodríguez-Yoldi, M. J.; Martínez-Beamonte, R.; Osada, J. Squalene through Its Post-Squalene Metabolites Is a Modulator of Hepatic Transcriptome in Rabbits. *Int. J. Mol. Sci.* **2022**, *23* (8), 4172.

(69) Agnihotri, S. A.; Mallikarjuna, N. N.; Aminabhavi, T. M. Recent advances on chitosan-based micro-and nanoparticles in drug delivery. *Journal of controlled release* **2004**, *100* (1), 5−28.

(70) Janes, K. A.; Fresneau, M. P.; Marazuela, A.; Fabra, A.; Alonso, M. a. J. Chitosan nanoparticles as delivery systems for doxorubicin. *Journal of controlled Release* **2001**, *73* (2−3), 255−267.

(71) Singh, A.; Mittal, A.; Benjakul, S. Chitosan nanoparticles: Preparation, food applications and health benefits. *Sci. Asia* **2021**, *47* (2021), 1−10.

(72) Vllasaliu, D.; Exposito-Harris, R.; Heras, A.; Casettari, L.; Garnett, M.; Illum, L.; Stolnik, S. Tight junction modulation by chitosan nanoparticles: comparison with chitosan solution. *International journal of pharmaceutics* **2010**, *400* (1−2), 183−193.

(73) Panyam, J.; Sahoo, S. K.; Prabha, S.; Bargar, T.; Labhasetwar, V. Fluorescence and electron microscopy probes for cellular and tissue uptake of poly (D, L-lactide-co-glycolide) nanoparticles. *International journal of pharmaceutics* **2003**, *262* (1−2), 1−11.

(74) Sahoo, S. K.; Panyam, J.; Prabha, S.; Labhasetwar, V. Residual polyvinyl alcohol associated with poly (D, L-lactide-co-glycolide) nanoparticles affects their physical properties and cellular uptake. *Journal of controlled release* **2002**, *82* (1), 105−114.

(75) Panyam, J.; Zhou, W. Z.; Prabha, S.; Sahoo, S. K.; Labhasetwar, V. Rapid endo-lysosomal escape of poly (DL-lactide-coglycolide) nanoparticles: implications for drug and gene delivery. *FASEB J.* **2002**, *16* (10), 1217−1226.

(76) Silva, A. M.; Alvarado, H. L.; Abrego, G.; Martins-Gomes, C.; Garduño-Ramirez, M. L.; García, M. L.; Calpena, A. C.; Souto, E. B. In vitro cytotoxicity of oleanolic/ursolic acids-loaded in PLGA nanoparticles in different cell lines. *Pharmaceutics* **2019**, *11* (8), 362.

(77) Rakotoarisoa, M.; Angelov, B.; Garamus, V. M.; Angelova, A. Curcumin-and fish oil-loaded spongosome and cubosome nanoparticles with neuroprotective potential against H2O2-induced oxidative stress in differentiated human SH-SY5Y cells. *ACS omega* **2019**, *4* (2), 3061−3073.

(78) Rinaudo, M. Chitin and chitosan: Properties and applications. *Prog. Polym. Sci.* **2006**, *31* (7), 603−632.

(79) Chattopadhyay, D.; Inamdar, M. S. Aqueous behaviour of chitosan. *Int. J. Polym. Sci.* **2010**, *2010*, 1.

(80) Abuobeid, R.; Herrera-Marcos, L. V.; Arnal, C.; Bidooki, S. H.; Sánchez-Marco, J.; Lasheras, R.; Surra, J. C.; Rodríguez-Yoldi, M. J.; Martínez-Beamonte, R.; Osada, J. Differentially Expressed Genes in Response to a Squalene-Supplemented Diet Are Accurate Discriminants of Porcine Non-Alcoholic Steatohepatitis. *International Journal of Molecular Sciences* **2023**, *24* (16), 12552.

(81) Kohno, Y.; Egawa, Y.; Itoh, S.; Nagaoka, S.-i.; Takahashi, M.; Mukai, K. Kinetic study of quenching reaction of singlet oxygen and scavenging reaction of free radical by squalene in n-butanol. *Biochimica et Biophysica Acta (BBA)-Lipids and Lipid Metabolism* **1995**, *1256* (1), 52−56.

(82) Sánchez-Marco, J.; Bidooki, S. H.; Abuobeid, R.; Barranquero, C.; Herrero-Continente, T.; Arnal, C.; Martínez-Beamonte, R.; Lasheras, R.; Surra, J. C.; Navarro, M. A.; et al. Thioredoxin domain containing 5 is involved in the hepatic storage of squalene into lipid droplets in a sex-specific way. *J. Nutr. Biochem.* **2024**, *124*, 109503.

(83) Bidooki, S. H.; Sánchez-Marco, J.; Martínez-Beamonte, R.; Herrero-Continente, T.; Navarro, M. A.; Rodríguez-Yoldi, M. J.; Osada, J. Endoplasmic Reticulum Protein TXNDC5 Interacts with PRDX6 and HSPA9 to Regulate Glutathione Metabolism and Lipid Peroxidation in the Hepatic AML12 Cell Line. *International Journal of Molecular Sciences* **2023**, *24* (24), 17131.

(84) Cárdeno, A.; Aparicio-Soto, M.; Montserrat-de la Paz, S.; Bermúdez, B.; Muriana, F. J.; Alarcón-de-la-Lastra, C. Squalene targets pro-and anti-inflammatory mediators and pathways to modulate over-activation of neutrophils, monocytes and macrophages. *Journal of Functional Foods* **2015**, *14*, 779−790.

(85) Lee, S.-O.; Jin, U.-H.; Kang, J. H.; Kim, S. B.; Guthrie, A. S.; Sreevalsan, S.; Lee, J.-S.; Safe, S. The orphan nuclear receptor NR4A1 (Nur77) regulates oxidative and endoplasmic reticulum stress in pancreatic cancer cells. *Molecular Cancer Research* **2014**, *12* (4), 527−538.

(86) Gu, M.-X.; Fu, Y.; Sun, X.-L.; Ding, Y.-Z.; Li, C.-H.; Pang, W.; Pan, S.; Zhu, Y. Proteomic analysis of endothelial lipid rafts reveals a novel role of statins in antioxidation. *J. Proteome Res.* **2012**, *11* (4), 2365−2373.

(87) Duivenvoorden, W.; Hopmans, S. N.; Austin, R. C.; Pinthus, J. H. Endoplasmic reticulum protein ERp46 in prostate adenocarcinoma. *Oncology Letters* **2017**, *13* (5), 3624−3630.